Hidden double excitations in the oxygen inner-shell ionization continuum of CO

R Püttner, D Céolin, O Travnikova, J Palaudoux, M Hoshino, H Kato, H Tanaka, Y Tamenori, C.C. Wang, C Miron, et al.

PAPER • OPEN ACCESS

Hidden double excitations in the oxygen inner-shell ionization continuum of CO

To cite this article: R Püttner *et al* 2013 *New J. Phys.* **15** 033003

New Journal of Physics
The open access journal for physics

Hidden double excitations in the oxygen inner-shell ionization continuum of CO

R Püttner[1,8], D Céolin[2], O Travnikova[2], J Palaudoux[3], M Hoshino[4], H Kato[4], H Tanaka[4], Y Tamenori[5], C C Wang[6], C Miron[2], K Ueda[6] and M N Piancastelli[3,7]

[1] Institut für Experimentalphysik, Freie Universität Berlin, D-14195 Berlin, Germany
[2] Synchrotron SOLEIL, l'Orme des Merisiers, Saint-Aubin, F-91192 Gif-sur-Yvette Cedex, France
[3] Université Pierre et Marie Curie, Laboratoire de Chimie Physique, Matière et Rayonnement (UMR7614), F-75231 Paris Cedex 05, France
[4] Department of Physics, Sophia University, Tokyo 102-8554, Japan
[5] Japan Synchrotron Radiation Research Institute, Sayo-gun, Hyogo 679-5198, Japan
[6] Institute of Multidisciplinary Research for Advanced Materials, Tohoku University, Sendai 980-8577, Japan
[7] Department of Physics and Astronomy, Uppsala University, SE-75120 Uppsala, Sweden
E-mail: ralph.puettner@fu-berlin.de

New Journal of Physics **15** (2013) 033003 (13pp)
Received 12 November 2012
Published 4 March 2013
Online at http://www.njp.org/
doi:10.1088/1367-2630/15/3/033003

Abstract. Auger decay spectra of CO subsequent to O 1s ionization with 549.85 eV photons, i.e. close to the top of the shape resonance, are presented. Their comparison with the normal Auger spectrum recorded at a photon energy well above the shape resonance reveals distinct features. In particular, in the energy region of the O $1s^{-1} \rightarrow b^1\Pi$ and O $1s^{-1} \rightarrow a^1\Sigma^+$ Auger transitions which are well known to consist of vibrational progressions, additional narrow lines are revealed by the spectra recorded at 549.85 eV. In a detailed fit analysis of these Auger spectra it was possible to show that the newly found lines do not exhibit

[8] Author to whom any correspondence should be addressed.

the expected distortions caused by post-collision interaction. This observation identifies these lines as caused by a different mechanism, such as resonant Auger decay processes of doubly excited states. The transitions are assigned using energy and intensity arguments in combination with complementary angular distribution measurements for the Auger electrons.

Contents

1. Introduction

Core-level photoelectron spectroscopy experiments provide a deep insight into symmetry and photoionization dynamics, see, e.g., [1–6]. Especially important for core-level spectroscopy is resonant excitation, which provides a well-defined (in energy and symmetry) intermediate state [7, 8]. While the most common experiments involve photoexcitation below a photoionization threshold, a wealth of resonant phenomena takes place also in the photoionization continuum. Of the resonant processes inherent to molecular core photoexcitation, perhaps the most commonly studied and utilized are the so-called shape resonances, which are one-electron effects in the continua, just above core-level ionization thresholds. Their apparent simplicity, large energy widths and well-defined symmetries have made shape resonances a popular area of study in molecular science [9–13] and a common tool for probing condensed-phase systems (e.g. adsorbates) [14–16]. The study of molecular shape resonances has not been without controversy (see, e.g., [12]). One central topic of debate concerned the detailed assignment of spectroscopic features above a core-level ionization threshold, especially the discernment of shape resonances from other resonant or non-resonant processes. A key point feeding the controversy is the difficulty unambiguously distinguishing shape resonances from either doubly excited states, which can be present above an ionization threshold and frequently overlap with shape resonances [12, 17, 18]. While there have been methods developed to distinguish between shape resonances and doubly or even triply excited states in absorption-type measurements, namely partial ion yield spectroscopy [17–19], less attention has been paid in the literature to the observation of decay processes following excitation in the spectral region of both shape resonances and doubly excited states. In particular, for the resonant Auger decay of doubly excited states only transitions to the low-lying two-hole one-particle (2h1p) final states were investigated [20]; in these cases there is no overlap of the normal and the resonant Auger spectra.

In this work, we describe a different approach, and namely we perform a very detailed analysis of the spectra in the normal Auger region of CO subsequent to O 1s photoionization. These spectra were obtained with the best possible resolution available nowadays and measured on top of the shape resonance and at a much higher photon energy. The data analysis is based on a very careful fitting procedure described in [21, 22] and takes into account, e.g., that the

shape resonance causes a redistribution on the vibrational structure of the photoelectron main line [23, 24]. As a consequence of this non-Franck–Condon effect on the vibrational distribution of the main line the presence of a shape resonance induces a definite change in the Auger decay spectra [25].

As a result of our approach, we were able to separate spectral features overlapping in kinetic energy into contributions which originate from normal and resonant Auger processes. In addition, we were able to identify the initial doubly excited and the final ionized state of the resonant Auger process. The final state turned out to be a highly excited 2h1p state which is energetically above the energy region studied with photoelectron spectroscopy so far.

2. Experimental setup and data analysis

A first series of experiments concerning the Auger spectra has been carried out on the c branch of the soft x-ray photochemistry beamline 27SU at SPring-8 in Japan [26]. The radiation source is a figure-8 undulator that can provide horizontally and vertically polarized light [27]. The monochromator installed on this branch is of Hettrick type [28] and provides monochromatic soft x-rays with the bandwidth of $\cong$50 meV in the O 1s excitation region. The high-resolution electron spectroscopy system employed consists of an SES-2002 hemispherical electron energy analyser, a gas cell and a differentially pumped main chamber [29]. The lens axis of the analyser is in the horizontal direction, whereas the entrance slit of the analyser is set parallel to the photon beam direction.

A second series of experiments, including the repetition of the Auger electron spectra (AES) and the measurement of complementary high-resolution O 1s photoelectron spectra (PES), was carried out on the soft x-ray beamline PLEIADES [31, 32] at the SOLEIL synchrotron in France. The radiation source is an elliptical undulator delivering linearly or elliptically polarized light in the range 35–1000 eV. The beamline is equipped with an in-house designed high-resolution plane grating monochromator with varied line spacing and varied groove depth gratings. The photoelectron and Auger spectra were recorded with a high-resolution VG Scienta R4000 spectrometer using a detection angle of 54.7° relative to the polarization of the synchrotron radiation. The total instrumental broadening for the Auger spectra was about 80 meV, resulting from the electron spectrometer resolution of 62 meV at 50 eV pass energy and a translational Doppler broadening of 53 meV. For the corresponding photoelectron spectrum recorded at 550 eV (600 eV) the total instrumental broadening was $\cong$60 meV ($\cong$70 meV), consisting of 25 meV electron spectrometer resolution at 20 eV pass energy, 55 meV (60 meV) photon energy broadening and 6 meV (18 meV) translational Doppler broadening. For the normalization of the electron spectra, the acquisition time, gas pressure and photon flux were taken into account.

To obtain an exact energy calibration in the photon energy region around 550 eV the total ion-yield spectrum of the O 1s $\rightarrow 2\pi$ excitation was recorded and calibrated to the values given by Püttner *et al* [30]; in this way an accuracy of better than 0.1 eV was obtained for the photon energy scale. Since the photoionization cross section is structureless around 600 eV no special efforts were made for an exact energy calibration in this photon energy region. Nevertheless, we expect that the accuracy of the photon energy is comparable to the above given value of 0.1 eV. The kinetic energies of the Auger spectra were calibrated with an accuracy of 60 meV by comparing the energy positions obtained in the fit analysis for the transitions O $1s^{-1} \rightarrow b^1\Pi$ and O $1s^{-1} \rightarrow a^1\Sigma^+$ with the values reported in [21].

The symmetry-resolved ion-yield spectra were also measured at beamline 27SU of the synchrotron radiation facility SPring8 using two identical retarding-potential-type ion detectors [33]. These detectors were mounted to fragment ions emitted parallel or perpendicular to the polarization direction of the light, i.e. transitions to states with Σ and Π symmetry, respectively. The spectra were calibrated using the energy values of the Rydberg excitations presented in [30].

The analysis of the present spectra is based directly on the analysis presented in a previous work on the Auger spectra of CO by some of the present authors [21]. The basic ideas of the data analysis are described in [22] and the specifications for CO in [21]; here we summarize only the major ideas and describe the differences from the procedure used in [21, 22]. The Franck–Condon factors (FCF) for the vibrational progressions of the Auger transitions are calculated by using an algorithm based on the work of Halmann and Laulicht [34] as well as Ory *et al* [35]. In this algorithm the electronic states are described with Morse potentials by using for the ground state the vibrational energy, $\hbar\omega$, the anharmonicity, $x\hbar\omega$, and the equilibrium distance, R_e, given in [36] and for the O 1s core-ionized state as well as the dicationic finals states $a^1\Sigma^+$, $b^1\Pi$ and $A^3\Sigma^+$ the values from our previous work [21].

In the fit procedure, post-collision interaction (PCI) was taken into account using for the direct terms in the Kramers–Heisenberg formula the lineshape given by Armen *et al* [37]. For the less important lifetime-interference terms, we used the lineshape given by the corresponding terms of the Kramers–Heisenberg formula by including an average energy shift due to the PCI effect; this shift amounts to 95 meV (25 meV) for the spectrum recorded at $h\nu = 549.85$ eV (600 eV). All spectra are convoluted with a Gaussian lineshape using the widths given above to simulate the experimental resolution.

Further details and, in particular, modifications of the fit approach necessary for the 549.85 eV spectrum are presented below along with a discussion of the spectra.

3. Results and discussion

Figure 1 shows the O 1s Auger spectrum of CO in the kinetic-energy range between 484 and 502 eV measured at SOLEIL using a photon energy of (a) 549.85 eV and (b) 600 eV. The photon energy of 549.85 eV is a result of a measurement with a nominal photon energy of 550 eV and a subsequent energy calibration. This value is a good compromise between being close to the broad maximum of the photoionization cross section (see the 54.7° spectrum in figure 2) and avoiding significant contributions of the normal Auger decay of the first O 1s satellite state which has its maximum slightly above 550 eV, see [38]. However, figure 2 shows that at 551 eV the σ-like shape resonance in the 0° spectrum overlaps with a maximum in the 90° spectrum. A comparison of the latter spectrum with the partial ion-yield spectrum of O^- presented by Stolte *et al* [17] clearly suggests that a broad peak at 551 eV detected under 90° is due to doubly excited states with Π-symmetry.

A comparison of the two spectra shown in figure 1 shows that the three additional features indicated with arrows are only present in the 549.85 eV spectrum. Based on the assignment of the spectral features present in the angularly resolved total ion yield spectra in figure 2 these spectral features can be due to three different contributions, as discussed before. Firstly, it is well known that across a shape resonance there are variations in the population of the different vibrational substates in the core-ionized state, see e.g. [24], which also led to changes in the Auger spectrum as has been shown in [25]. Secondly, the lower kinetic energy of the

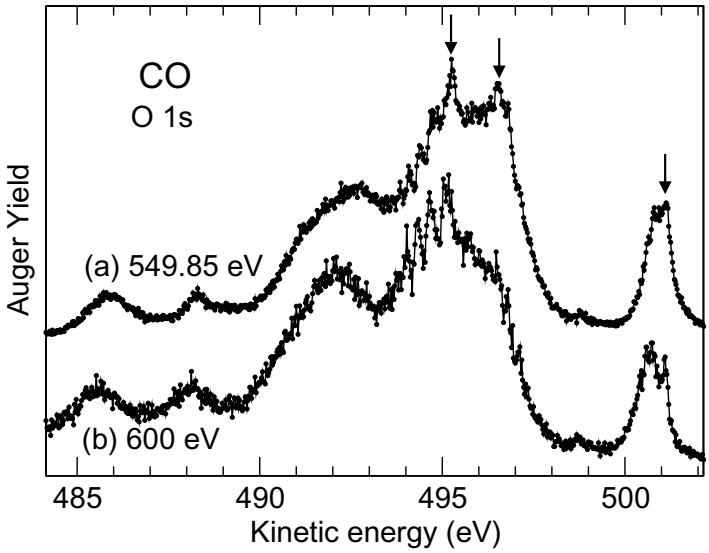

Figure 1. O 1s Auger spectrum of CO in the kinetic-energy region between 484 and 502 eV measured at a photon energy of (a) 549.85 eV and (b) 600 eV. Three spectral features, which are only visible in the spectrum measured at 549.85 eV, are marked by vertical arrows.

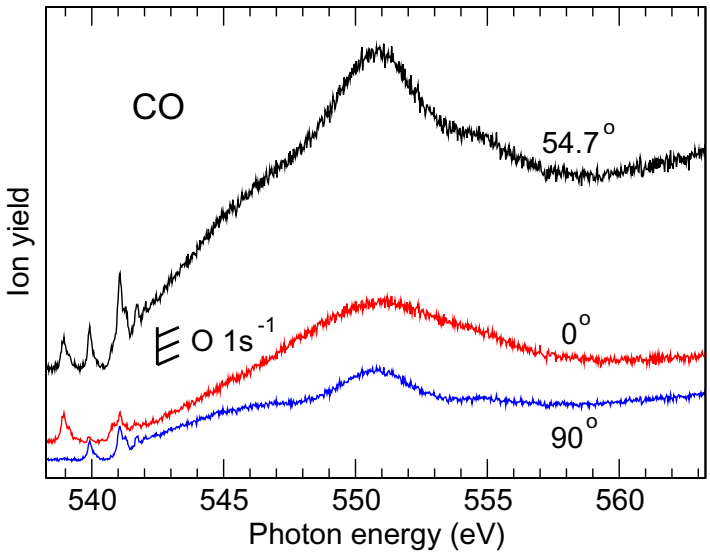

Figure 2. The symmetry-resolved O 1*s* ion-yield spectrum of CO. The spectral components corresponding to perpendicular transitions [$I_{\mathrm{ion}}(90^\circ)$], i.e. with final states of Π-symmetry, and parallel transitions [$I_{\mathrm{ion}}(0^\circ)$], i.e. with final states of Σ-symmetry, are shown by the blue and the red spectrum, respectively. The total ion-yield spectrum at magic angle [$I_{\mathrm{ion}}(54.7^\circ)$] obtained using the equation $2 \cdot I_{\mathrm{ion}}(90^\circ) + I_{\mathrm{ion}}(0^\circ)$ is displayed in black. For a better visibility of the spectra their baselines of zero intensity are shifted relative to each other.

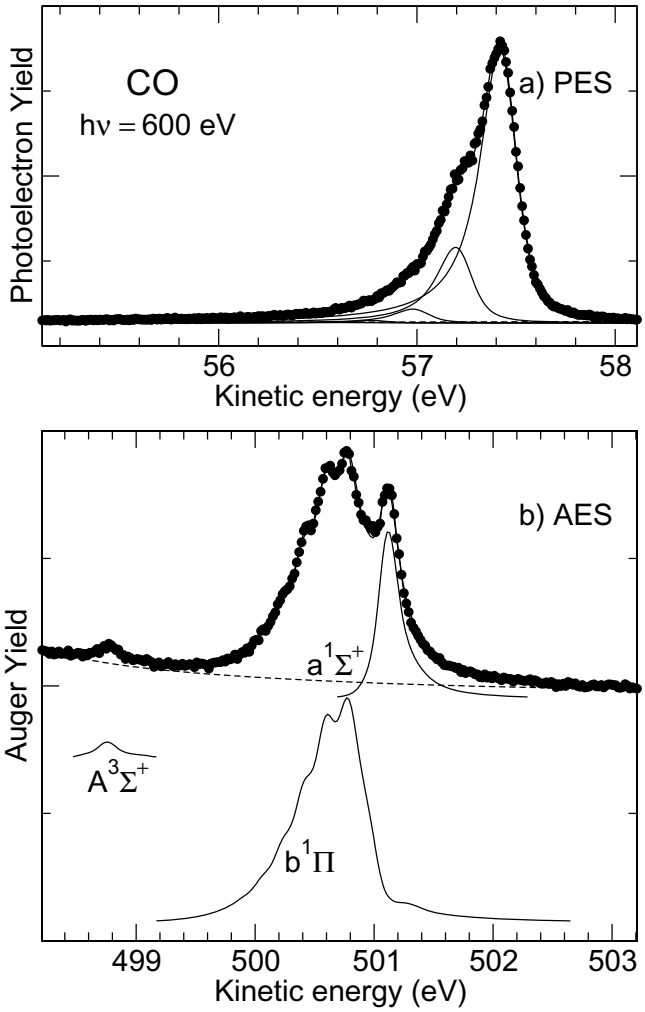

Figure 3. (a) Photoelectron and (b) Auger spectra recorded at a photon energy of 600 eV. In both spectra, the solid lines through the data points represent the fit results and the dashed lines indicate the background. In the PES the subspectra represent the different vibrational substates of the core-ionized state, while in the AES the subspectra indicate the vibrational progressions of the Auger decays to the final states $a^1\Sigma^+$, $b^1\Pi$ and $A^3\Sigma^+$.

photoelectron at a photon energy of 549.85 eV leads to a strongly increased PCI effect. Thirdly, a contribution of resonant Auger lines caused by the decay of the doubly excited states can be expected.

To distinguish between these three different possible contributions, we analyse in detail the Auger spectrum in the kinetic energy region 498.2–503.2 eV, i.e. the region with the O $1s^{-1} \rightarrow b^1\Pi$ and O $1s^{-1} \rightarrow a^1\Sigma^+$ Auger transitions. The spectra recorded with photon energies of 600 and 549.85 eV are shown in figures 3 and 4, respectively, together with the corresponding photoelectron spectra. As described above, the data analysis of the photoelectron and Auger spectra measured at 600 eV is identical to that used by Püttner *et al* [21]. However, to reduce the number of free parameters in the fit analysis, the parameters for the potential energy curves

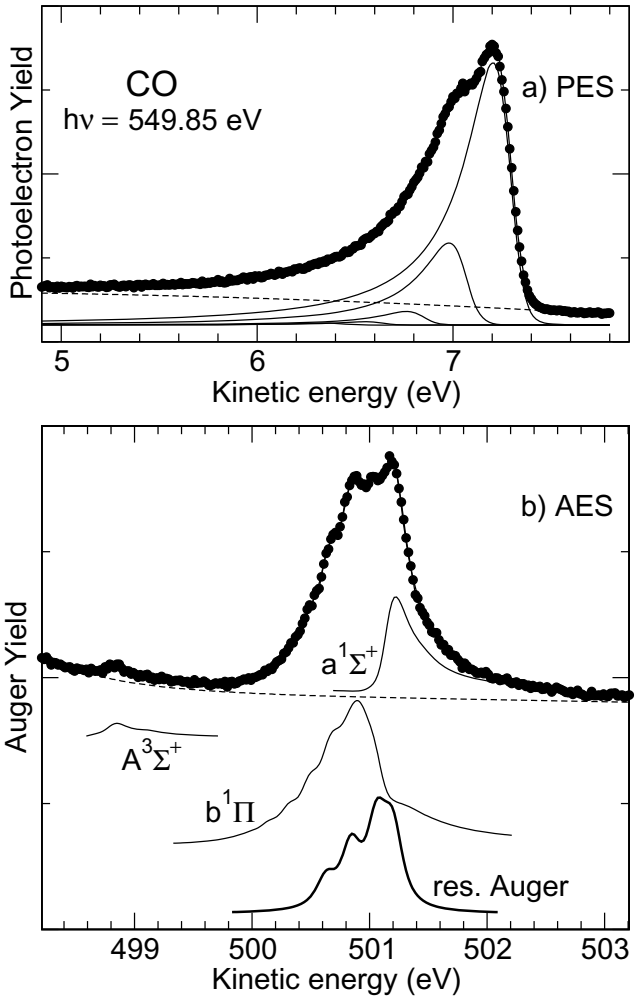

Figure 4. (a) Photoelectron and (b) Auger spectra recorded at a photon energy of 549.85 eV. The bold solid subspectrum in the AES represents the contributions of the resonant Auger decays of the doubly excited state. For more details, see figure 3.

and the energetic splittings were fixed to the values reported in [21] and only the intensities were allowed to vary freely. As can be seen in figure 3 the fit result describes the data well and the intensity ratios turned out to be identical within the error bars to the results of the previous work.

For the fit analysis of the 549.85 eV spectrum presented in figure 4 we took into account the stronger contributions of the PCI effect, which is reflected by more asymmetric lines in the photoelectron and Auger spectra. Furthermore, we performed a fit of the photoelectron spectrum using the same potential energy curves—and therefore the same FCF—as for the spectrum recorded using a photon energy of 600 eV. To account for the influence of the shape resonance described above, all higher vibrational substates were multiplied with a weight factor. In the fit analysis it turned out that the weight factors for the vibrational levels $v = 1$ and 2 are 1.15 and 1.05, respectively, i.e. there are only small variations of the intensities of the vibrational substates caused by the shape resonance. These weight factors for the individual vibrational

substates were also used in the Auger spectrum in order to take into account the influence of the shape resonance on the photoionization process. The influence of the PCI effect and the shape resonance on the spectrum can be seen from the differences in the vibrational progressions of the O $1s^{-1} \rightarrow b^1\Pi$ and O $1s^{-1} \rightarrow a^1\Sigma^+$ Auger transitions, i.e. the thin solid subspectra in figures 3 and 4. However, as can be seen from the fit results, the modifications caused by the PCI effect and the shape resonance were not sufficient for a good description of the 549.85 eV spectrum. Instead, four additional PCI lineshapes had to be included between 500.3 and 501 eV, shown by bold lines in figure 4. For these PCI lineshapes the kinetic energy of the corresponding photoelectron was a free parameter during the fit analysis and it turned out to be of the order of 600 eV, with an error bar of 300 eV. This result shows that a PCI tail is practically absent in the additionally included lines. This excludes the Auger decay of the lowest O $1s^{-1}$ satellite state that cannot be fully rejected from pure energy arguments alone [38], and allows to identify that they originate from a resonant Auger decay of a doubly excited state.

The four narrow lines indicate that both the doubly excited and the final state involved in the corresponding transition are stable with respect to dissociation. The postulation of a doubly excited state that is stable with respect to dissociation is not in contradiction with the absence of a vibrational progression in the total ion yield spectra owing to two reasons: (i) the vibrational splittings in O 1s excitations of CO are generally comparable to the core-hole lifetime [30]. Because of this, e.g., the vibrational progression of the O $1s \rightarrow 2\pi$ excitation below threshold is only weakly visible [30]. Slightly smaller vibrational energies would smear out the vibrational progression almost completely. (ii) An overlap of spectral features caused by the excitation of different doubly excited states might mask vibrational progressions in the angular resolved total ion yield spectra.

The four observed lines show splittings between 140 and 210 meV, i.e. in the order typical of vibrational splittings. The irregularities in the splittings might be due to various effects. Firstly, the vibrational level of the doubly excited state is not known and a population of two almost overlapping vibrational states is possible. Such situations can lead to a complicated vibrational pattern including vibrational lifetime interference. Secondly, the vibrational progressions can be influenced by an avoided crossing.

The resonant Auger decay of the doubly excited state leads to an excited state of CO^+. The latter state has an energy of 48.9 eV above the ground state of CO and can be described as a 2h1p state. Since neither experimental nor theoretical studies of excited CO^+ exist above 46 eV [39], the assignment of this state is not straightforward. For an approach to the assignment we will, therefore, use in a first step simple energy arguments. These arguments are based on the energies of the two-hole (2h) states, which are for the states of interest not known with high accuracy. Because of this, we would like to point out that inaccuracies of 1–2 eV for their energy positions do not have consequences for the following discussion.

Using the energies of the 2h states obtained in the combined experimental and theoretical work of Kelber *et al* [40], one can exclude the 2h configurations $5\sigma^{-1}1\pi^{-1}$, $5\sigma^{-2}$, $4\sigma^{-1}5\sigma^{-1}$ and $1\pi^{-2}$ since the corresponding states are too low in energy. Assuming the 2h configuration $4\sigma^{-1}1\pi^{-1}$ with an energy of $\cong$51 eV above the ground state of CO, the 2h1p final state could be $4\sigma^{-1}1\pi^{-1}nl\lambda$, with $nl\lambda$ describing a Rydberg orbital. In this case the additional Rydberg electron would have a binding energy of 2–3 eV. This allows one to estimate n by comparing with the binding energies of the Rydberg electrons obtained by Kitajima *et al* [20] in combination with the Rydberg formula. In this way, we obtain $n = 5$–6. In the same way one can obtain $n = 3$ for the state $4\sigma^{-2}nl\lambda$, since the $4\sigma^{-2}$ parent state is expected to be around

58 eV, i.e. the binding energy of the additional Rydberg electron is ≅9 eV. For the parent state $3\sigma^{-1}5\sigma^{-1}$ the binding energy of the additional electron would be ≅17 eV and for the parent states $3\sigma^{-1}4\sigma^{-1}$ and $3\sigma^{-1}1\pi^{-1}$ ≅25 eV. These binding energies are clearly too high for an additional Rydberg electron. However, Sundin *et al* [41] observed that the states $5\sigma^{-1}1\pi^{-1}2\pi$, $5\sigma^{-2}2\pi$ and $4\sigma^{-1}5\sigma^{-1}2\pi$ are approximately 18 eV below the corresponding parent states so that an assignment of the present 2h1p state to $3\sigma^{-1}5\sigma^{-1}2\pi$ would be reasonable based on energy arguments.

In summary, the presented energy arguments suggest the assignments $4\sigma^{-1}1\pi^{-1}5, 6l\lambda$, $4\sigma^{-2}3l\lambda$, or $3\sigma^{-1}5\sigma^{-1}2\pi$. From these possible assignments the first one can be excluded by considering the double excitation process in more detail. The relatively high contribution of the resonant Auger decay to the spectrum can only be explained with an effective excitation process to the doubly excited state. This would be preferentially accompanied by a conjugate shake process of a 4σ or 1π valence electron to a Rydberg state with the principal quantum number $n = 5$ or 6; such a process is, however, not very likely based on overlap arguments for valence electrons with high-n Rydberg electrons.

As discussed above, the narrow lines of the additional spectral feature match a vibrational progression well and suggest that the final state is stable with respect to dissociation. This finding can be explained much better by the final state $4\sigma^{-2}3l\lambda$ than by the final state $3\sigma^{-1}5\sigma^{-1}2\pi$, since in the former case two electrons are missing in the antibonding 4σ orbital and the additional electron is in a non-bonding Rydberg orbital. Contrary to this, the second remaining possibility, the state $3\sigma^{-1}5\sigma^{-1}2\pi$, has only vacancies in the bonding orbitals 3σ and 5σ and an additional electron in the antibonding 2π orbital, suggesting a much stronger weakening of the bond.

The doubly excited state formed by an O 1s $\rightarrow 2\pi$ excitation and an additional shake process has Π symmetry, see above. To obtain the proposed final state $4\sigma^{-2}3l\lambda$ the 2π electron has to be involved in a participator Auger decay. Under these conditions the first hole in the 4σ orbital has to be created already in the excitation process. Consequently, the doubly excited state has to be formed by a conjugate shake process starting from the 4σ orbital, i.e. the doubly excited state is O $1s^{-1}4\sigma^{-1}2\pi 3l\sigma$, forming the final state $4\sigma^{-2}3l\sigma$. In the subsequent participator Auger decay the excited 2π and the remaining 4σ electron are involved and in this way the second hole in the 4σ orbital is created. From the present considerations, we cannot determine the angular momentum l of the Rydberg electron.

The present assignment of the final state to $4\sigma^{-2}3l\sigma$ without a further specification of l is supported by the overview spectra for the O 1s Auger decay. By comparing the Auger spectra recorded at 549.85 and 600 eV an additional spectral feature can also be found in the 549.85 eV spectrum at about 4.5 and 6 eV above the $4\sigma^{-2}3l\sigma$ state, see arrows. In the following, we shall show that these splittings are in line with the formation of a Rydberg series $4\sigma^{-2}nl\sigma$ with n = 3–5 and l being more likely s than p. Kitajima *et al* [20] and Sundin *et al* [41] showed that the states $5\sigma^{-2}3s\sigma$ and $4\sigma^{-1}5\sigma^{-1}3s\sigma$ are approximately 9.5 eV below the corresponding threshold. Using this energy value, i.e. by assuming the lowest 2h1p final state to be $4\sigma^{-2}3s\sigma$, we calculated on the basis of the Rydberg formula that the states $4\sigma^{-2}4s\sigma$ and $4\sigma^{-2}5s\sigma$ are higher by 4.7 and 6.6 eV, respectively. The states $5\sigma^{-2}3p\pi$ and $4\sigma^{-1}5\sigma^{-1}3p\pi$ are only 7.5 eV below the corresponding threshold [20, 41]. By assuming identical binding energies for a $3p\sigma$ Rydberg electron, we obtained that the states $4\sigma^{-2}4p\sigma$ and $4\sigma^{-2}5p\sigma$ are higher by 3.5 and 5.0 eV, respectively. These considerations suggest that all additional spectral features in the Auger spectrum recorded at 549.85 eV form a Rydberg series. The formation of

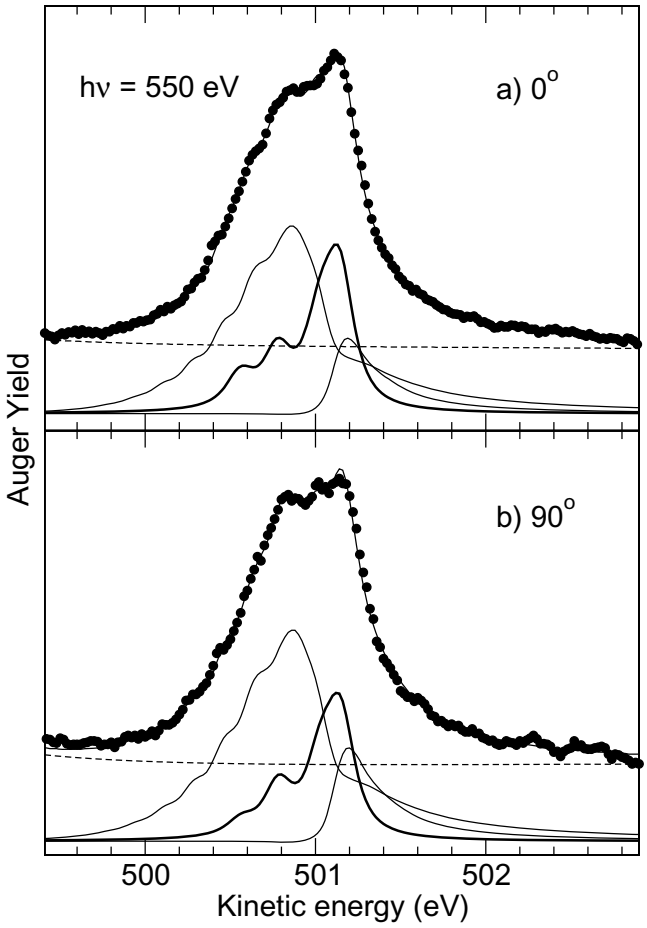

Figure 5. The Auger spectrum in the energy region from 499.4 to 502.9 eV subsequent to an ionization with 550 eV photons measured at an angle of (a) 0° and (b) 90° relative to the polarization of the light. The solid line through the data points represents the fit result. The thin solid subspectra represent the O $1s^{-1} \rightarrow a^1\Sigma^+$ and O $1s^{-1} \rightarrow b^1\Pi$ normal Auger transitions, the bold solid subspectrum the resonant Auger transitions and the dashed subspectrum the background.

the Rydberg series can readily be explained by shake-up transitions of the $3l\lambda$ Rydberg electron accompanying the resonant Auger process. Furthermore, the values for the energy splitting fit better the series $4\sigma^{-2}ns\sigma$ so that this assignment is preferred.

This proposed assignment is also in line with the angularly resolved Auger spectra recorded at SPring 8 with a nominal photon energy of $h\nu = 550$ eV and depicted in figure 5; for these spectra no proper photon energy calibration was performed. However, the contributions of the resonant Auger decays in these spectra match very well those of the spectra recorded at $h\nu = 549.85$ eV and indicate clearly that the photon energies used for these two spectra differ by not more than 0.1 eV.

In Auger spectra recorded on the C 1s shape resonance of CO it has been observed that different Auger transitions may exhibit different angular distributions [42]. However, in the two present angularly resolved spectra the intensity ratio for the normal Auger decays to the final

states $a^1\Sigma^+$ and $b^1\Pi$ is identical within the error bars, i.e. both Auger transitions show the same angular distribution behaviour. Because of this, we can use the intensities of the normal Auger lines as a reference, and we observe that the contributions of the resonant Auger lines are in the horizontal spectrum 1.4(1) times more intense than in the vertical spectrum. The higher contributions of the resonant Auger lines in the 0° spectrum can be understood qualitatively on the basis of the given assignment and suggested participator Auger decay. According to the assigned Π symmetry of the doubly excited state, the preferred orientation of the molecular axis is perpendicular to the polarization of the light. According to the assignment of the final state to a Σ symmetry the outgoing Auger electron has to have π symmetry, i.e. it goes out mainly perpendicular to the molecular axis. Using the following argumentation, we can qualitatively understand the relative 1.4:1 intensity ratio for the 0°- and the 90°-detection. For this argumentation let us assume that the polarization direction of the light and the 0°-detector is along the z-axis and that of the 90°-detector is along the x-axis. Then the doubly excited molecule can be oriented along the x- or the y-axis. In the case of an orientation along the x-axis there will be an Auger emission along the y- and the z-axis, i.e. there will be a signal only in the 0°-detector. For an orientation in the y-axis there will be a signal in both detectors so that the total intensity ratio is about 2:1 and shows the same tendency as the observation. Using similar arguments, one obtains for a possible sσ continuum wave equal intensity in both detectors and for a pσ continuum wave intensity only in the 90°-detector.

4. Summary and conclusions

We report here a very detailed analysis of Auger structures measured after O $1s^{-1}$ photoionization in CO at photon energies corresponding either to the continuum shape resonance or well above such a maximum in the photoionization cross section. Based on a sophisticated fitting procedure, taking into account the vibrational progression of the normal Auger spectra as well as their modifications caused by several factors such as PCI and vibrational distribution on and off the shape resonance, we were able to evidence the presence of additional spectral features overlapping with the normal Auger ones at the shape resonance position. On the basis of their lineshapes as well as their energy and electron angular distribution behaviour, we were able to assign these spectral features as being related to the resonant Auger decay of doubly excited states, which happen to overlap in energy with the shape resonance. Energy, intensity and symmetry arguments allowed us to propose a spectral assignment of the doubly excited state to O $1s^{-1}4\sigma^{-1}2\pi 3l\lambda$ and of the 2h1p final state to $4\sigma^{-2}3l\sigma$ of CO^+, both with l = s or p. The state of CO^+ is energetically 48.9 eV above the ground state of CO, i.e. above the energy range up to 46 eV investigated with photoelectron spectroscopy [39].

Up to now, resonant Auger transitions were systematically studied only in the kinetic-energy regime below that of the normal Auger transitions. From this work, we conclude that by combining state-of-the-art experimental resolution and advanced fitting procedures, we are able to disentangle a complex decay process following photoexcitation to neutral doubly excited states happening to overlap with a shape resonance, which is, in the present case, the CO photoionization continuum above the O $1s^{-1}$ threshold. Such analyses should allow us to study highly excited 2h1p states of molecular ions which overlap in Auger spectra with the low-lying dicationic states and which have not yet been observed with photoelectron spectroscopy directly. Moreover, the present approach is not limited by the selection rules for the photoionization

process allowing only ionic states with Σ and Π symmetry. As shown here, this approach requires neither assigned nor clearly resolved doubly excited states.

Acknowledgments

The measurements at SPring-8 were carried out with the approval of the SPring-8 programme advisory committee and supported in part by Grants-in-Aid for Scientific Research from the Japan Society for the Promotion of Science and by Matsuo Foundation. We are grateful to the staff at SPring-8 for their help. At SOLEIL Synchrotron (France), the experiment was performed at the PLEIADES beamline during the beamtime allotted under proposal number 99110013. We are grateful to E Robert for technical assistance and to the staff of SOLEIL for stable operation of the equipment and storage ring during the experiments. This work was supported by the European Union Seventh Framework Program FP7/2007-2013 under grant agreement no. 252781 (to OT). MNP acknowledges the French Agence Nationale de la Recherche (ANR) for financial support in the framework of a 'Chair d'Excellence' programme. The analysis in Berlin was supported by the Deutsche Forschungsgemeinschaft under project no. PU180/6-1.

References

[1] Eberhardt W 1987 *Phys. Scr.* **T17** 28
[2] Hanson D 1990 *Adv. Chem. Phys.* **77** 1
[3] Svensson S, Aksela H and Aksela S 1995 *J. Electron Spectrosc. Relat. Phenom.* **75** 67
[4] Nenner I and Morin P 1996 *VUV and Soft X-Ray Photoionization* ed U Becker and D Shirley (New York: Plenum) p 291
[5] Piancastelli M N 2000 *J. Electron Spectrosc. Relat. Phenom.* **107** 1
[6] Miron C and Morin P 2011 *Handbook of High-Resolution Spectroscopy* vol 3 (New York: Wiley) pp 1655–89
[7] Feifel R and Piancastelli M N 2011 *J. Electron Spectrosc. Relat. Phenom.* **183** 10 and references therein
[8] Piancastelli M N, Hempelmann A, Heiser F, Gessner O, Rüdel A and Becker U 1999 *Phys. Rev.* A **59** 300
[9] Hemmers O, Heiser F, Eiben J, Wehlitz R and Becker U 1993 *Phys. Rev. Lett.* **71** 987
[10] Neeb M, Rubensson J-E, Biermann M and Eberhardt W 1993 *Phys. Rev. Lett.* **71** 3091
[11] Schmidbauer M, Kilcoyne A L D, Köppe H-M, Feldhaus J and Bradshaw A M 1995 *Phys. Rev.* A **52** 2095
[12] Piancastelli M N 1999 *J. Electron Spectrosc. Relat. Phenom.* **100** 167
[13] Côté R, Dalgarno A, Lyyra A M and Li L 1999 *Phys. Rev.* A **60** 2063
[14] Paolucci G, Surman M, Prince K C, Sorba L, Bradshaw A M, McConville C F and Woodruff D P 1986 *Phys. Rev.* B **34** 1340
[15] Stöhr J 1992 *NEXAFS Spectroscopy* (Berlin: Springer)
[16] Budau P and Raseev G 1995 *Phys. Rev.* B **51** 16993
[17] Stolte W C, Hansen D L, Piancastelli M N, Dominguez Lopez I, Rizvi A, Hemmers O, Wang H, Schlachter A S, Lubell M S and Lindle D W 2001 *Phys. Rev. Lett.* **86** 4504
[18] Yu S-W, Stolte W C, Guillemin R, Öhrwall G, Tran I C, Piancastelli M N, Feng R and Lindle D W 2004 *J. Phys. B: At. Mol. Opt. Phys.* **37** 3583
[19] Shigemasa E, Gejo T, Nagasono M, Hatsui T and Kosugi N 2002 *Phys. Rev.* A **66** 022508
[20] Kitajima M *et al* 2008 *Phys. Rev.* A **78** 033422
[21] Püttner R, Liu X-J, Fukuzawa H, Tanaka T, Hoshino M, Tanaka H, Harries J, Tamenori Y, Carravetta V and Ueda K 2007 *Chem. Phys. Lett.* **445** 6
[22] Püttner R, Hu Y F, Bancroft G M, Aksela H, Nõmmiste E, Karvonen J, Kivimäki A and Aksela S 1999 *Phys. Rev.* A **59** 4438
[23] Hergenhahn U, Kugeler O, Rüdel A, Rennie E E and Bradshaw A M 2001 *J. Phys. Chem.* **105** 5704

[24] Mistrov D A, De Fanis A, Kitajima M, Hoshino M, Shindo H, Tanaka T, Tamenori Y, Tanaka H, Pavlychev A A and Ueda K 2003 *Phys. Rev.* A **68** 022508
[25] Sorensen S L, Miron C, Feifel R, Piancastelli M N, Björneholm O and Svensson S 2008 *Chem. Phys. Lett.* **456** 1
[26] Ohashi H, Ishiguro E, Tamenori Y, Kishimoto H, Tanaka M, Irie M and Ishikawa T 2001 *Nucl. Instrum. Methods* A **467** 529
[27] Tanaka T and Kitamura H 1996 *J. Synchrotron Radiat.* **3** 47
[28] Ohashi H *et al* 2001 *Nucl. Instrum. Methods* A **468** 533
[29] Shimizu Y *et al* 2001 *J. Electron Spectrosc. Relat. Phenom.* **114-116** 63
[30] Püttner R, Dominquez I, Morgan T J, Cisneros C, Fink R F, Rotenberg E, Warwick T, Domke M, Kaindl G and Schlachter A S 1999 *Phys. Rev.* A **59** 3415
[31] Miron C *et al* www.synchrotron-soleil.fr/Recherche/LignesLumiere/PLEIADES
[32] Lindblad A, Kimberg V, Söderström J, Nicolas C, Travnikova O, Kosugi N, Gel'mukhanov F and Miron C 2012 *New J. Phys.* **14** 113018
[33] Saito N *et al* 2000 *Phys. Rev.* A **62** 042503
[34] Halmann M and Laulicht I 1965 *J. Chem. Phys.* **43** 438
[35] Ory H A, Gittelman A P and Maddox J P 1964 *Astrophys. J.* **139** 346
[36] Herzberg G 1950 *Molecular Spectra and Molecular Structure I. Spectra of Diatomic Molecules* (New York: Van Nostrand) p 522
[37] Armen G B, Tulkki J, Åberg T and Crasemann B 1987 *Phys. Rev.* A **36** 5606
[38] Ehara M, Kuramoto K, Nakatsuji H, Hoshino M, Tanaka T, Kitajima M, Tanaka H, De Fanis A, Tamenori Y and Ueda K 2006 *J. Chem. Phys.* **125** 114304
[39] Baltzer P, Lundqvist M, Wannberg B, Karlsson L, Larsson M, Heyes M A, West J B, Siggel M R F, Parr A C and Dehmer J L 1994 *J. Phys. B: At. Mol. Opt. Phys.* **37** 4915
[40] Kelber J A, Jennison D R and Rye R R 1981 *J. Chem. Phys.* **75** 652
[41] Sundin S, Sorensen S L, Ausmees A, Björneholm O, Hjelte I, Kikas A and Svensson S 1999 *J. Phys. B: At. Mol. Opt. Phys.* **32** 267
[42] Hemmers O, Heiser F, Eiben J, Wehlitz R and Becker U 1994 *Nucl. Instrum. Meth.* B **87** 209